

## Biocompatible poly(vinylidene fluoride)/cyanoacrylate composite coatings with tunable hydrophobicity and bonding strength

I. S. Bayer,<sup>1,a)</sup> M. K. Tiwari,<sup>2</sup> and C. M. Megaridis<sup>2,b)</sup>

<sup>1</sup>Department of Aerospace Engineering, University of Illinois at Urbana-Champaign, Urbana, Illinois 61801, USA

<sup>2</sup>Department of Mechanical and Industrial Engineering, University of Illinois at Chicago, Chicago, Illinois 60607, USA

(Received 6 September 2008; accepted 4 October 2008; published online 31 October 2008)

Biocompatible composite coatings are produced from solution processable poly(vinylidene fluoride)/cyanoacrylate blends prepared in the presence of rosin and ZnO particle fillers, the latter for control of coating surface microstructure. Dispersions are spray coated and cured at 100 °C onto aluminum foils and fiberglass cloths suitable for tissue engineering applications. The elastic modulus of the composite films matches or exceeds that of polyethylene-based orthopedic implant materials. Contact angle measurements on coated fiberglass cloths reveal that wettability of hydrophobic coatings is maintained under strain for applied mechanical stress levels up to ~15 kN/m<sup>2</sup>, whereas ultrahydrophobic coatings fail at ~5 kN/m<sup>2</sup>. © 2008 American Institute of Physics. [DOI: 10.1063/1.3009292]

Poly(vinylidene fluoride) (PVDF) is a polymer with exceptional chemical resistance, thermal stability, and outstanding dielectric and piezoelectric properties, which justify its widespread use as ultrafiltration and microfiltration membrane material,<sup>1–4</sup> in lithium ion batteries,<sup>5</sup> and in developing organic/inorganic or all-organic electromechanical composite materials.<sup>6,7</sup> Being a biocompatible polymer, PVDF has been used to prepare special bioactive surfaces facilitating cellular proliferation and adhesion in human osteogenesis,<sup>8</sup> in soft tissue applications, and as a suture material.<sup>9</sup> However, in applications where surface adhesion is critical, use of PVDF poses a challenge due to its inherent hydrophobicity and chemical inertness against functionalization. Hence, blends of PVDF with suitable acrylic resins have been developed, which improve PVDF's pigment wetting and coating adhesion. Poly(methyl methacrylate) (PMMA) and PVDF are completely miscible in the molten state.<sup>10</sup> However, PMMA is not an electromechanically active polymer. Thus, in applications where electromechanical properties of PVDF are critical, the presence of PMMA can be disadvantageous. A highly functional and biocompatible class of acrylics, known as cyanoacrylates (CAs) (superglue), offers an attractive alternative for enhancing adhesion of PVDF blends. The cyano (C≡N) group present in CA monomer is electroactive, having ferroelectric functionality,<sup>11</sup> which makes CAs highly suitable as bone fillers, enabling enhanced osteobonding and new bone growth<sup>12</sup> due to polarization of the cyano group.<sup>13</sup> Furthermore, CAs display superior adhesion strength compared to other acrylics and they cure rapidly in biomedically favorable moist environments. In this letter, we describe solvent-processed fabrication of flexible coatings comprising PVDF and CA blend polymer matrix with tunable microstructure and hydrophobicity. Application-specific variations in surface wettability and microstructure are achieved by adding functional micro- and nanostructured fillers into the polymer blend.

PVDF is not processable with most industrial solvents. Dimethyl formamide (DMF) is the most common solvent for PVDF. However, DMF acts as a catalyst for rapid polymerization of CA monomer in solution, thus making DMF unsuitable for blending CA with PVDF. It is known that the presence of weak acids in solution can help control or even hinder CA polymerization;<sup>14</sup> however, incorporation of acids in multicomponent polymer solutions can cause dispersion instability and unwanted reactions. We found that rosin inhibits CA polymerization in solution even in the presence of DMF and is miscible with CA in solution. This could be due to the fact that abietic acid, which naturally occurs in rosin, is a weak carboxylic acid.<sup>15</sup>

PVDF/CA blends were prepared in the presence of rosin. Methyl ethyl ketone dispersed CA monomer (2-ethylcyanoacrylate, Sigma-Aldrich, USA) was directly blended with rosin (Sigma-Aldrich, USA) stock solution consisting of 60 wt % rosin in isopropyl alcohol/castor oil (7/1 in weight) solvent. When the PVDF in DMF solution was added to the mixture, no spontaneous polymerization of CA monomer was observed. The blends were adjusted such that a hydrophobic PVDF/CA/rosin weight ratio of 6/3/1 was maintained in solution. Three different forms of ZnO fillers, i.e., zinc oxide (ZnO) microparticles (~5 μm, Sigma-Aldrich, USA) or dry (ZnO) nanopowder (~70 nm, Alfa-Aesar, USA) or a commercial surface functionalized ZnO nanodispersion (NanoTek, 50 wt %, 70 nm, Alfa-Aesar, USA), were used. Surface functionalization of ZnO was achieved by encapsulating the particles with hydrophilic polyhydroxylated macromolecules (long-chain glycols). Coatings were spray cast using an industrial grade internal mix airbrush atomizer (IWATA, USA). Polished aluminum foil and a highly hydrophilic two-dimensional yarn fiberglass cloth (mass density of 0.075 kg/m<sup>2</sup>, BGF Industries, USA) were used as substrates.

Figure 1(a) shows an aluminum foil coated with a film containing 7 wt % functionalized ZnO nanoparticles dispersed in CA/rosin (3/1 weight) solution and no PVDF. The cured (~85 °C in open air for ½ h) coating caused the initially flat foil to coil up. The contraction of the film is caused

<sup>a)</sup>Electronic mail: ibayer1@illinois.edu.

<sup>b)</sup>Electronic mail: cmm@uic.edu.

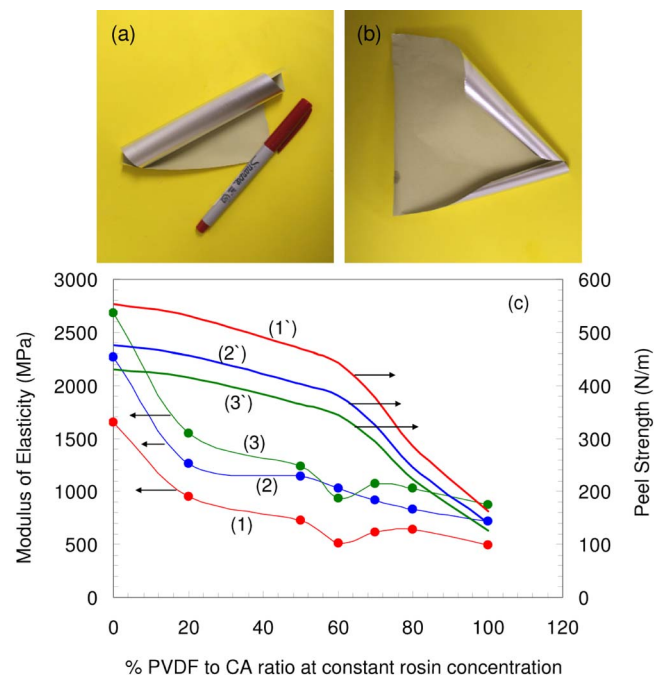


FIG. 1. (Color online) (a) Aluminum foil coated with CA/rosin (3/1 weight) dispersion containing 7 wt % functionalized ZnO and no PVDF. (b) Aluminum foil coated with PVDF/CA/rosin (5/4/1 weight) dispersion containing 7 wt % functionalized ZnO. (c) Change in elastic modulus and peel strength of nanocomposite coatings as a function of PVDF/CA blend weight ratio and ZnO concentration. Curves: [(1) and (1')] 2 wt % ZnO, [(2) and (2')] 6 wt % ZnO, and [(3) and (3')] 8 wt % ZnO concentration. The overall rosin concentration in all the coatings was  $\sim 12$  wt %.

by rapid cross-linking of the CA monomer upon thermosetting. The cohesive cross-linking (cause for contraction) strength of acrylic matrices upon curing can reach  $\sim 10$  MPa.<sup>16</sup> CA polymerization cohesive strength is even higher, i.e.,  $\sim 25$  MPa,<sup>17</sup> thus causing the film to be stiff and brittle. For another coating containing PVDF (PVDF/CA/rosin, 5/4/1 weight), the rollup of the substrate could be largely reduced, as shown in Fig. 1(b). The linear PVDF polymer chains can interfere with the CA cross-linking, thus modifying the elastic modulus of the composite. In addition, cross-linking of CA with the PVDF matrix should reduce the PVDF crystallite sizes and increase the intercrystallite entanglements causing the formation of a rubbery state within the composite.<sup>18</sup> This change in elasticity of the nanocomposite films was studied with the help of measurements presented in Fig. 1(c). The change in modulus of elasticity was measured as a function of PVDF/CA blend weight ratio. The rosin content was  $\sim 12$  wt % in all cases. An Instron 5540 tensile tester was used with 400  $\mu\text{m}$  thick cast film specimens. Curves (1)–(3) in Fig. 1(c) show the elastic modulus of the nanocomposite coatings to increase with the concentration of functionalized ZnO nanoparticles in the range of 2–8 wt %. Pure CA/ZnO composites (0% PVDF/CA ratio) were very stiff; as PVDF was added and its concentration increased, the modulus of elasticity of the coatings declined by more than 50%, suggesting more flexible composites in the presence of PVDF. Ultrahigh molecular weight polyethylene (UHMWPE), which is widely used as a load-bearing orthopedic implant, has a modulus with elasticity of  $\sim 1000$  MPa.<sup>19</sup> The PVDF/CA based composites appear to match or exceed the elastic properties of UHMWPE in addition to being easily solution processable. Figure 1(c) also

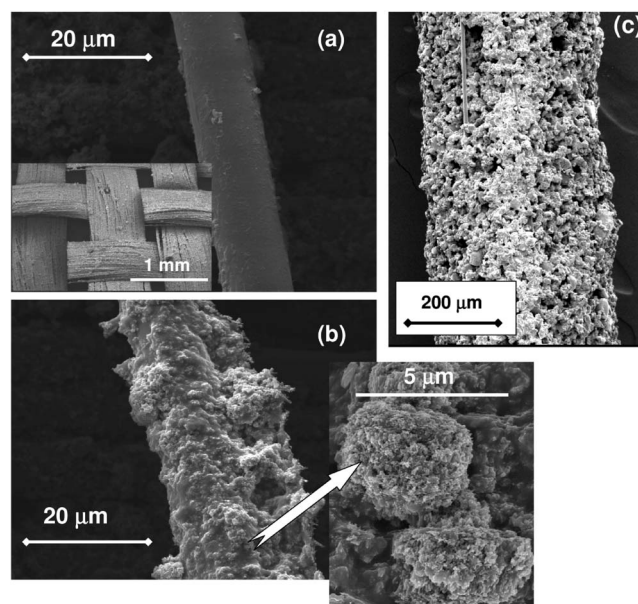


FIG. 2. SEM micrographs of (a) uncoated glass fiber of approximately 10  $\mu\text{m}$  in diameter. The inset shows the morphology of the coated glass-fiber yarn using dry ZnO nanopowder. (b) Coated glass fibers isolated from the fiberglass cloth. The magnified detail shows the surface micro-/nanoscale morphology of the coating. (c) A bundle of glass fibers with a microporous PVDF/CA/rosin coating filled with unmodified ZnO microparticles ( $\sim 5$   $\mu\text{m}$ , 8 wt %).

shows the estimated peel strengths<sup>20</sup> of the composite coatings on a polished smooth aluminum surface. Two separate regions of peel strength are apparent, namely, a regime of low sensitivity to PVDF concentration (up to 60 wt %) and, above 60 wt %, a regime of higher sensitivity. Estimated peel strength values of the present composites with less than 60 wt % PVDF match or exceed commercial aluminum composite panels containing modified polyester/PVDF blends ( $\sim 400$  N/m) or PVDF surfaces modified by plasma enhanced graft copolymerization techniques.<sup>21</sup>

Meshlike fiberglass-based materials have been recently applied as scaffolds for hard-soft interface regeneration<sup>22</sup> in tissue engineering. Surface morphology, mechanical properties, and adhesion characteristics of such scaffolds are critical to maintain continuous hard-soft interface regeneration in tissue engineering. The present biocompatible coatings can also be applied onto such scaffolds to induce additional interface functionality, such as porosity control, antimicrobial activity, and adhesion strength manipulation. Figure 2(a) shows a scanning electron microscopy (SEM) image of an uncoated glass fiber ( $\sim 10$   $\mu\text{m}$  in diameter) isolated from a hydrophilic fiberglass cloth. The inset in Fig. 2(a) shows a coated fiberglass cloth sample. The SEM image in Fig. 2(b) shows the morphology of the dry ZnO nanopowder-filled PVDF/CA/rosin coating on a glass fiber separated from the yarn. As seen, the coating introduces both micro- and nano-scale roughness on the fiberglass substrate [see magnified detail in Fig. 2(b)], thus rendering the fiber hydrophobic. Morphology of the coating was manipulated by adjusting the weight fraction of the unmodified ZnO nanopowder used. At ZnO powder concentrations above  $\sim 9$  wt %, surfaces were superhydrophobic (water contact angle of  $>150^\circ$ ) due to the increased surface roughness of the hydrophobic coatings;<sup>23</sup> however, adhesion to the fiberglass cloth decreased considerably. To increase the porosity of the scaffold, micron-sized

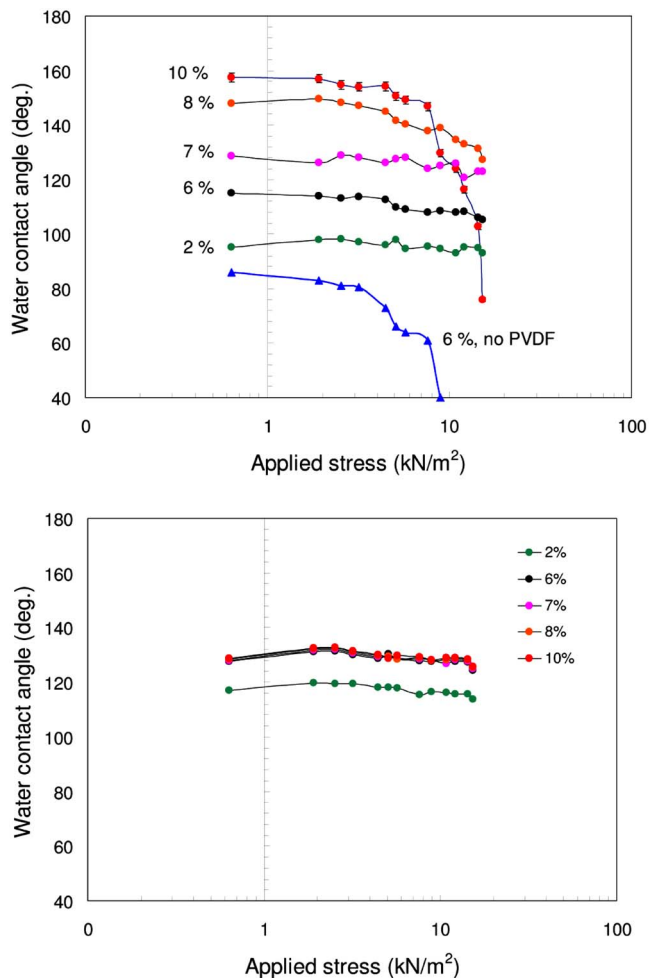


FIG. 3. (Color online) Sessile water contact angle variation as a function of applied tensile stress. (a) Coatings containing unmodified ZnO nanopowder. The reductions in contact angle were accompanied by flaking of coatings under mechanical stress. The coatings withstood 3–5 kN/m<sup>2</sup> depending on their composition. (b) Coatings containing functionalized ZnO. The contact angle is nearly insensitive to ZnO concentration beyond 6 wt %.

ZnO fillers were used. In Fig. 2(c), a SEM image of a microporous PVDF/CA/rosin coating applied over a bundle of glass fibers is shown. Due to micron-sized fillers, hydrophobicity of the coatings declined by  $\sim 45^\circ$  as water contact angles indicated.

To assess the dependence of bonding strength and wettability of the composite coatings to the fiberglass cloth surface under mechanical strain, a horizontal tensile tester (Tinius Olsen, USA) was used. Figure 3(a) shows the contact angle change with applied stress for the coatings on fiberglass using unmodified ZnO nanoparticle fillers. The contact angles appear to stay nearly constant for applied stresses up to 3 kN/m<sup>2</sup> for all samples. Wettability of the coating without PVDF degraded at the lowest threshold stress (marked by subsequent precipitous reduction in contact angle), as this coating was stiff and brittle. The coatings containing PVDF showed higher contact angle at the lowest stress (practically the same as the stress-free condition) for the same concentration of ZnO due to the hydrophobic nature of PVDF [compare the two curves for 6% in Fig. 3(a)]. The highest contact angle measured for these coatings was 158°. The coatings containing PVDF show good durability up to 5 kN/m<sup>2</sup> even at 10 wt % ZnO nanopowder concentration. However, due to poor dispersion of ZnO nanoparticles—particularly above

7 wt %—the coatings showed signs of flaking and deterioration of contact angle at high stresses.

Figure 3(b) shows the results for composite containing functionalized ZnO nanoparticles. Wetting of the coated surfaces remained nearly unchanged for stress values up to 15 kN/m<sup>2</sup> even for 10 wt % particle loading. This indicates that the coatings withstood higher stress rates without peeling off from the substrate. It is argued that better dispersion of the functionalized nanoparticles within the polymer matrix, as compared to unmodified ZnO, enables efficient polymer chain mobility, hence improving strain resistance. In addition, efficient nanoparticle dispersion within the polymer matrix can transform large PVDF spherulites into thin fiber-like crystallites, thus causing better energy dissipation within the polymer matrix. Better dispersed functionalized nanoparticles decreased the coating hydrophobicity probably by diminishing hierarchical surface roughness.

In conclusion, a low-cost ZnO filled PVDF/CA composite fabrication technique was demonstrated. The surface wettability and microstructure of the composites were adjustable. The elastic modulus of the composites matched the UHMWPE ( $\sim 1000$  MPa), a common orthopedic implant material. Wettability of the composites containing surface modified ZnO nanoparticles withstood higher mechanical stress than composites containing unmodified ZnO nanoparticles. Dispersion of the unmodified nanoparticles within the polymer matrix ( $\sim 10$  wt %) formed hierarchical surface roughness, a necessary condition for superhydrophobicity. The mechanical integrity of the superhydrophobic coatings was lower.

<sup>1</sup>A. J. Lovinger, in *Developments in Crystalline Polymers*, edited by D. C. Bassett (Applied Science, London, 1982), p. 195.

<sup>2</sup>M. G. Broadhurst, G. T. Davis, J. E. McKinney, and R. E. Collins, *J. Appl. Phys.* **49**, 4992 (1978).

<sup>3</sup>T. Boccaccio, A. Bottino, G. Capannelli, and P. Piaggio, *J. Membr. Sci.* **210**, 315 (2002).

<sup>4</sup>L. Ying, E. T. Kang, and K. G. Neoh, *Langmuir* **18**, 6416 (2002).

<sup>5</sup>H. Li, J. Wei, F. Shan, J. Yang, and X. Wang, *J. Polym. Sci., Part B: Polym. Phys.* **46**, 751 (2008).

<sup>6</sup>T. S. Bayer, A. Biswas, J. B. Szczech, E. Suhir, and M. G. Norton, *Appl. Phys. Lett.* **92**, 083303 (2008).

<sup>7</sup>X. He and K. Yao, *Appl. Phys. Lett.* **89**, 112909 (2006).

<sup>8</sup>F. J. C. Braga, S. O. Rogero, A. A. Couto, R. F. C. Marques, A. A. Ribeiro, and J. S. C. Campos, *Mater. Res.* **10**, 247 (2007).

<sup>9</sup>U. Klinge, B. Klosterhalfen, A. P. Ottinger, K. Junge, and V. Schumpelick, *Biomaterials* **23**, 3487 (2002).

<sup>10</sup>R. E. Prud'Homme, *Polym. Eng. Sci.* **22**, 90 (1982).

<sup>11</sup>J. Dziaduszek, R. Dabrowski, K. Czuprynski, and N. Bennis, *Ferroelectrics* **343**, 3 (2006).

<sup>12</sup>S. Bhat, M. J. Askew, G. Njus, and D. J. Smith, *J. Appl. Biomater* **3**, 207 (1992).

<sup>13</sup>C. R. Bowen, J. Gittings, I. G. Turner, F. Baxter, and J. B. Chaudhuri, *Appl. Phys. Lett.* **89**, 132906 (2006).

<sup>14</sup>J. E. Schoenberg, U.S. Patent No. 4,182,823 (08 January 1980).

<sup>15</sup>J. S. Lee and S. I. Hong, *Eur. Polym. J.* **38**, 387 (2002).

<sup>16</sup>R. L. Sakaguchi, B. D. Wiltbank, and C. F. Murchison, *Dent. Mater.* **20**, 402 (2004).

<sup>17</sup>W. G. Repensek, in *Handbook of Adhesive Technology*, edited by A. Pizzi and K. L. Mittal (Dekker, New York, 2003), pp. 801–812.

<sup>18</sup>X. Zhou and M. Cakmak, *Polym. Eng. Sci.* **47**, 2110 (2007).

<sup>19</sup>S. Roy, S. Bag, and S. Pal, *Trends Biomater. Artif. Organs* **17**, 54 (2004).

<sup>20</sup>Z. Czech, *Int. J. Adhes. Adhes.* **26**, 414 (2006).

<sup>21</sup>Y. X. Liu, E. T. E. Kang, K. G. Neoh, K. L. Tan, C. C. Huan, and D. J. Liaw, *J. Adhes.* **17**, 35 (1999).

<sup>22</sup>I. Ahmed, M. Lewis, I. Olsen, and J. C. Knowles, *Biomaterials* **25**, 501 (2004).

<sup>23</sup>A. B. D. Cassie and S. Baxter, *Trans. Faraday Soc.* **40**, 546 (1944).